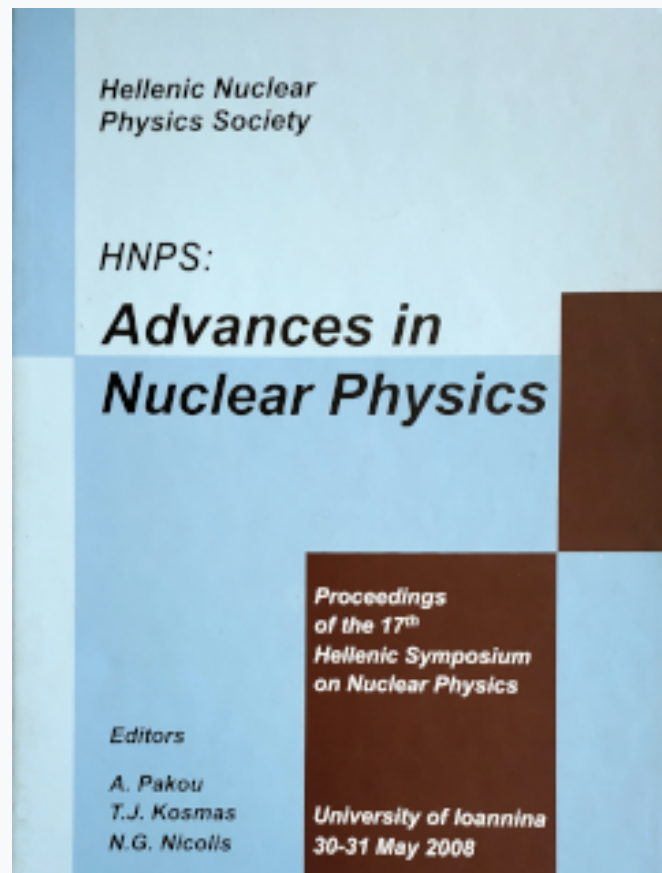


HNPS Advances in Nuclear Physics

Vol 16 (2008)

HNPS2008



The new external ion-beam station at the Demokritos Tandem 5.5 MV accelerator: A unique analytical tool in the fields of cultural heritage and environmental science

D. Sokaras, ... et al.

doi: [10.12681/hnps.2599](https://doi.org/10.12681/hnps.2599)

To cite this article:

Sokaras, D., & et al., . (2020). The new external ion-beam station at the Demokritos Tandem 5.5 MV accelerator: A unique analytical tool in the fields of cultural heritage and environmental science. *HNPS Advances in Nuclear Physics*, 16, 209–218. <https://doi.org/10.12681/hnps.2599>

The new external ion-beam station at the Demokritos Tandem 5.5 MV accelerator: A unique analytical tool in the fields of cultural heritage and environmental science

D. Sokaras¹, S. Karabagia¹, E. Bistekos¹, L. Georgiou¹,
J. Salomon², M. Bogovac³, A. Lagoyannis¹, S. Harissopoulos¹,
V. Kantarelou¹, E. Aloupi⁴, I. Aslani⁴, V. Paschalis⁵ and
A. G. Karydas¹

¹ *Institute of Nuclear Physics, NCSR "Demokritos", 15310, Athens, Greece*

² *Laboratoire du C2RMF, Centre de Recherche et de Restauration des Musées du France UMR 171 Palais du Louvre, 14, Quai François Mitterrand, 75001 Paris, France*

³ *Institute R. Boskovic, Zagreb, Croatia*

⁴ *Thetis Authentics Ltd, 41 M. Mousourou str., 11636 Athens Greece*

⁵ *Benaki Museum, 6 Hesiodou str. 10674 Athens Greece*

Abstract

At the 5.5 MV Tandem accelerator of the Institute of Nuclear Physics of NCSR Demokritos, Athens, a new external ion-beam set-up has been recently installed. The aim of this development was to establish a complete experimental set-up integrating the analytical capabilities of the PIXE, RBS and PIGE techniques, so that a complete elemental and near surface structural characterization of samples/artifacts to be attained in an almost non-destructive way and without any limitation concerning their size or conductive state. A careful 3D mechanical drawing optimized the experimental parameters of the set-up so that the special requirements imposed for optimum performance of the aforementioned techniques to be fulfilled. The first applications were focused in the quality control of tagged materials (technologically authentic replicas of attic ceramics and in coatings used by conservators for paintings).

1 Introduction

In our technologically highly developed society, ion beams have become indispensable: a host of applications ranging from medical therapy to the analysis of cultural heritage (CH) artifacts depend strongly on the use of ion beams. As a result of the advantages of the ion-beam analytical techniques, new accelerator-based research infrastructures have been established in some European countries with rich cultural heritage. A bright example hereby is the AGLAE accelerator laboratory in Paris [1]. Located under the Louvre Museum, the AGLAE accelerator provides state of the art analytical techniques and methodologies for the full characterization of cultural heritage artifacts by employing ion-beam methods for more than one decade. The basic idea of using ion beams for CH studies has recently been adopted by other countries too. Hence, two new accelerator laboratories dedicated to CH studies have been recently established, i.e. the LABEC accelerator laboratory in Florence, Italy [2,3] and the Centro Nacional de Aceleradores in Seville, Spain [4].

The extensive employment of ion beams in CH research, since the last 30 years, stems from the non-invasive and non-destructive effects they have on the archaeological artifacts and artworks during their analytical treatment, in particular if they are implemented in atmospheric pressure, as well as from their excellent analytical performance and capabilities. The synergy of ion-beam analytical methods, can provide elemental analysis of almost the whole periodic table as well as, in the case of a microbeam, excellent spatial resolution, laterally and in depth. These features are of key importance for the analysis of cultural materials that exhibit extremely diverse elemental composition and structure, as well as surface and depth inhomogeneities. The analysis of such materials requires setups with multi-elemental analytical ability and enhanced sensitivity. The aforementioned prerequisites can, e.g., be satisfied by integrating complementary analytical techniques in a single experimental setup that employs simultaneously Particle Induced X-Ray Emission (PIXE), Rutherford Backscattering Spectrometry (RBS), Nuclear Reaction Analysis (NRA) and Particle Induced Gamma-ray Emission (PIGE). Such a setup would provide unique analytical possibilities compared to conventional and traditional methods, i.e., fully implemented elemental analysis and structural characterization at the same time, and would also facilitate the development of new characterization methods for CH materials. It is worth mentioning that Particle Induced X-ray Emission, (PIXE) provides multi-elemental, simultaneous analysis of elements with atomic number ranging from $Z = 11$ (Sodium) to $Z = 92$ (Uranium), with lower limits of detection down to a few $\mu\text{g/g}$. Novel analytical procedures in PIXE analysis can also contribute towards in depth profiling studies. Furthermore, Rutherford Backscattering, (RBS), gives complementary quantitative information of most elements in stratified layers including also the case of low atomic number elements such as oxygen or carbon. Finally, Nuclear Reaction Analysis (NRA) is preferably applied to the determination

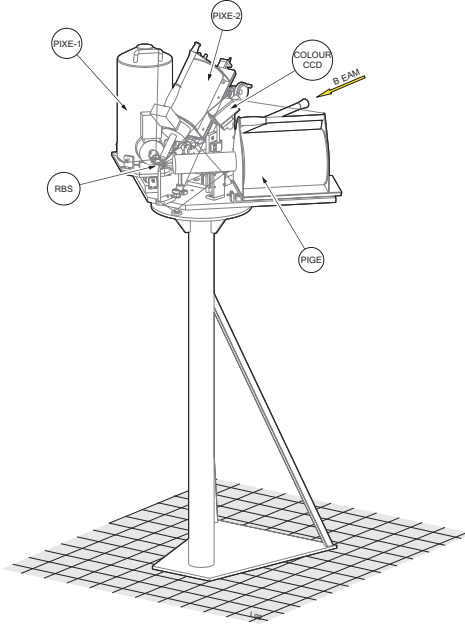


Fig. 1. 3D mechanical drawing of the Demokritos Tandem accelerator external beam set-up.

of the depth distribution of light elements ($Z \leq 16$) and especially to Hydrogen profiling measurements.

In the present paper we describe the development of Demokritos Tandem accelerator external beam line to be dedicated for analytical studies with relevance to the cultural heritage objects and environmental samples.

2 Development of the external ion beam set-up

The new external ion-beam setup utilizes simultaneously five detectors, two for the implementation of PIXE, one for RBS, one for PIGE, and one X-ray detector for the dose monitoring (Fig.1, Fig.2).

The exit ion-beam nozzle provides collimation and minimizes the beam dimensions (0.7mm) maintaining currents at least up to 5 nA in this way minimum damage and energy loss is produced at the exit window (selected to be a $100\text{ nm Si}_3\text{N}_4$ window) and in the air path between the window and sample position. The geometry arrangement of the detectors was optimally designed and installed in order to allow: 1) a simultaneous utilization of two X-ray detectors for PIXE measurements, the one being in He atmosphere and the other one with 'hard' filtering in order to achieve combined detection of major, minor and trace elements emitting X-rays with energy from 1 to 30 keV , 2) a surface barrier detector placed in vacuum inside a special constructed chamber for the RBS mode that enables characterization of a near surface layered struc-

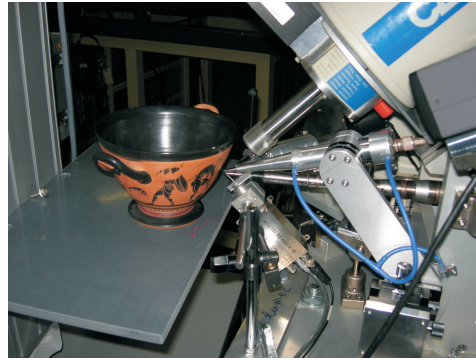


Fig. 2. The external beam station in Demokritos Tandem Laboratory.

tures or surfaces of depletion/enrichment of particular elements, 3) detection of prompt γ -rays induced by nuclear reaction on the isotopes of the low atomic number elements that compose the sample (Li, B, F, Na, Mg, Al, Si), 4) precise dose normalization by means of the $Si - K$ signal emanating from the Si_3N_4 exit window and 5) visual inspection of the analysis area and tools for easy and reproducible alignment of the sample/artifact with respect to the particle beam. For the data acquisition, two Xilinx XtremeDSP Development kits for Virtex-4 SX cards were used.

2.1 *The integrated beam set-up*

PIXE analysis: PIXE studies are achieved by means of the simultaneous utilization of two X-ray $Si(Li)$ detectors. One is used for the detection of low energy (1-8keV) X-rays (major/minor elements), using He atmosphere, so as to improve considerably the transmission efficiency of low energy X-rays. This detector is mounted at 135° with respect to the beam on the horizontal plane and is fitted with a magnetic deflector (Fig. 3), to avoid the entrance of backscattered particles, while He flows properly inside its detection channel. Another $Si(Li)$ detector is used for the detection of high energy X-rays (minor, trace elements). It is mounted at wider solid angle, at 135° on the vertical plane, utilizing a $140\mu m$ thick Kapton and a $50\mu m$ thick Al absorbers, for the strong filtering of low energy X-rays induced from the low atomic number elements and for absorbing completely the backscattered particles. In this way, the combined detection of major, minor and trace elements emitting X-rays with energy from 1 to 30keV can be achieved.

RBS analysis: A surface barrier, $300\mu m$, silicon detector is used for the detection of the backscattered particles. It is placed in a conical vacuum chamber at an angle of about 160° with respect to the beam axis and it is possible to approach a few mm away from the analysis point. In order to minimize the energy loss of the detected backscattered particles, $100nm$ of Si_3N_4 is used as chamber's entrance window providing in that way the best possible resolution

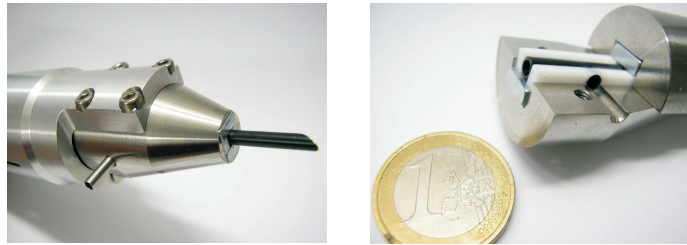


Fig. 3. Nozzle for the low-energy $Si(Li)$ detector including deflections magnets and channel for constant Helium flow.



Fig. 4. Conical vacuum chamber for the surface barrier detector utilized in RBS measurements.

for the RBS spectra.

PIGE analysis: A high purity germanium γ -ray detector can be mounted at 135° on the horizontal plane to detect γ -rays from nuclear reactions induced on light isotopes of elements contained in the sample.

2.2 Visual inspection and sample handling

Visual inspection of the analysis area is achieved using a CCD camera and two lasers for easy and reproducible alignment of the sample/artifact with respect to the particle beam and at the exact defined distance. Furthermore, for proper handling the sample/artifact is mounted on a x-y translation stage (Fig. 2).

2.3 Ion Beam exit nozzle/Collimation

The careful design of the exit ion-beam nozzle restricts beam dimensions to $\sim 0.7mm$, maintaining on the same time currents at least up to 10 nA and

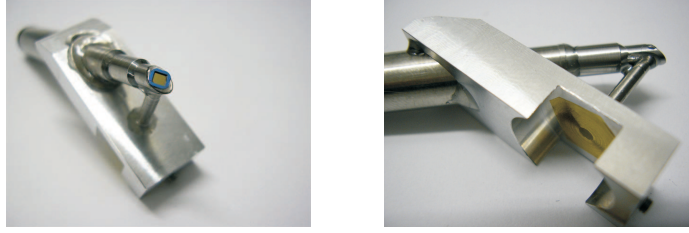


Fig. 5. Beam exit nozzle with the 100nm Si_3N_4 exit window.

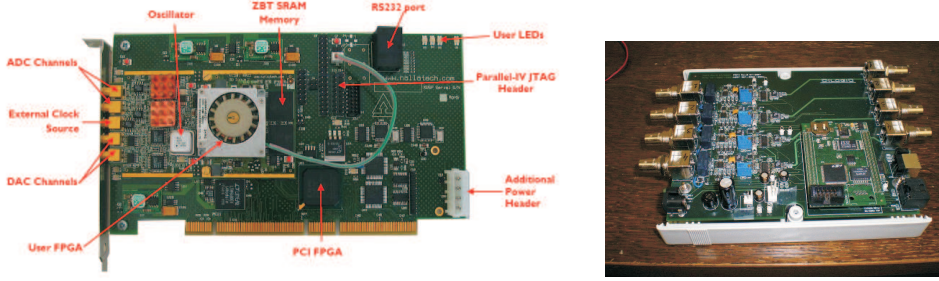


Fig. 6. Xilinx XtremeDSP and prefilter unit for DSP of four simultaneous spectrometers (two PIXE, RBS, PIGE).

inducing minimum energy loss at the exit window (100 nm Si_3N_4 window). At the same time the tiny size of the nozzle allows all the detection systems to approach optimally the analysis point offering this way maximum detection solid angles.

2.4 Charge measurement

Beam dose normalization is achieved by means of the $Si - K$ signal emanating from the 100nm Si_3N_4 exit ion-beam window (Fig. 5) with the use of a PIN diode detector, having a 25 μm thick Be window, mounted at 135° with respect to the beam axis.

2.5 Data Acquisition System

For the data acquisition, novel hardware and software tools were used to perform digital pulse processing. In particular, two Xilinx XtremeDSP Development kits for Virtex-4 SX cards (Fig. 6) were used as a complete platform for development of an on-chip digital pulse processor for X-ray, γ -ray and particle detectors. Each card accepts two analog signals from prefilter (Fig. 6) and performs digitization, shaping and recording using custom FPGA configuration.

| Proton Energy(<i>keV</i>) | 1500 | | 3000 | | 4000 | |
|--|------|-----|------|-----|------|----|
| Exit Window | Air | He | Air | He | Air | He |
| - | 78 | 14 | 33 | 7 | 19 | 5 |
| <i>Si₃N₄</i> (100nm) | 89 | 42 | 38 | 21 | 25 | 16 |
| Kapton (8μm) | 270 | 248 | 116 | 107 | 84 | 79 |

Table 1

Proton beam broadening in μm assuming a beam path of 8mm.

3 Analytical performance of the external ion beam set-up

3.1 Beam broadening due to scattering

The major factors limiting the spatial resolution of an external ion beam system is scattering by the exit window and by the molecules of the ambient gas. As shown in Table 1, scattering by the molecules of the ambient gas dominates when very thin exit windows are used (e.g. *Si₃N₄*), while for thicker windows the main cause of the beam spread is the window itself. Table 1 indicates that the usage of 100nm *Si₃N₄* results to the optimum possible resolution for the transmitted ion beam.

3.2 X-ray attenuation

Low energy X-rays (below 2keV) emitted from the sample are greatly attenuated by the surrounding gas. Fig. 7 indicates that the use of He atmosphere for the detection of low energy X-rays is essential, while for elements of high atomic number the analysis in air does not produce any significant decrease in the PIXE intensities.

3.3 Dose measurement precision

For testing precision and reproducibility of the dose measurement an *Al* foil was irradiated at different proton currents and the *Al* – *K* signal emanating from the foil, together with the *Si* – *K* signal emanating from the *Si₃N₄* beam exit window, were measured on the low energy *Si(Li)* detector and on the monitor PIN diode, respectively. In Fig. 8, the normalized *Al* – *K* intensity with respect to the *Si* – *K* intensity is plotted for different beam currents. The blue line is the mean value of the ratio of the two signals and the red spots are the data points. The data show excellent precision ($\sim 0.4\%$) in the

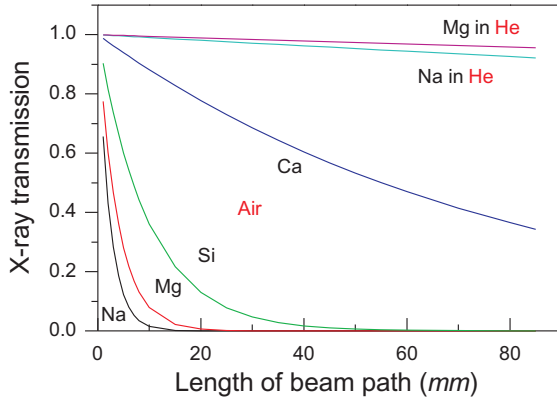


Fig. 7. Transmission for the corresponding characteristic x-ray line in Air and Helium.

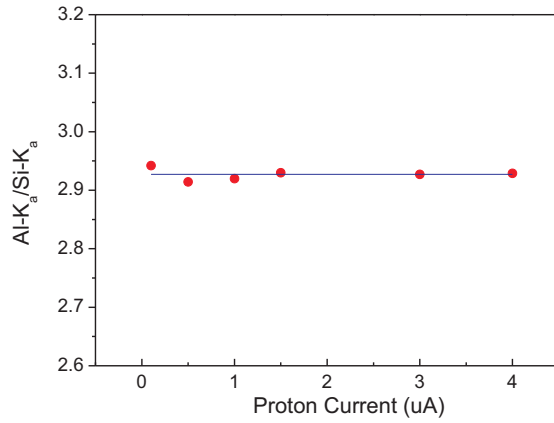


Fig. 8. Measurements for the dose-indication precision.

dose measurement.

4 Experimental - Preliminary measurements

The first measurements using the integrated external beam set-up were performed on standard reference materials and monoelemental targets. Fig. 9 compares two PIXE spectra from a certified reference material (BAM) which was irradiated with 3 MeV protons. The blue line indicates the PIXE spectra taken from the low energy detector, while the red curve is the PIXE spectra from the high energy detector. Table 2 shows the certified elemental concentrations of the specific material. In Fig. 9 a typical RBS spectrum taken from a $2\mu\text{m}$ thick Zn foil, irradiated with 1.5 MeV protons is also presented.

Table 2
Concentrations for the certified oxides of the reference glass BAM.

| Oxides | Concentration (ppm) |
|-----------------------|---------------------|
| Silicon (IV) oxide | 710000 |
| Sodium oxide | 137000 |
| Calcium oxide | 105000 |
| Magnesium oxide | 23000 |
| Aluminum oxide | 11000 |
| Potassium oxide | 7000 |
| Arsenic oxide | 132 |
| Copper (II) oxide | 112 |
| Iron (III) oxide | 422 |
| Molybdenum (VI) oxide | 343 |
| Lead (II) oxide | 202 |
| Strontium oxide | 151 |
| Zinc oxide | 203 |
| Zirconium (IV) oxide | 842 |

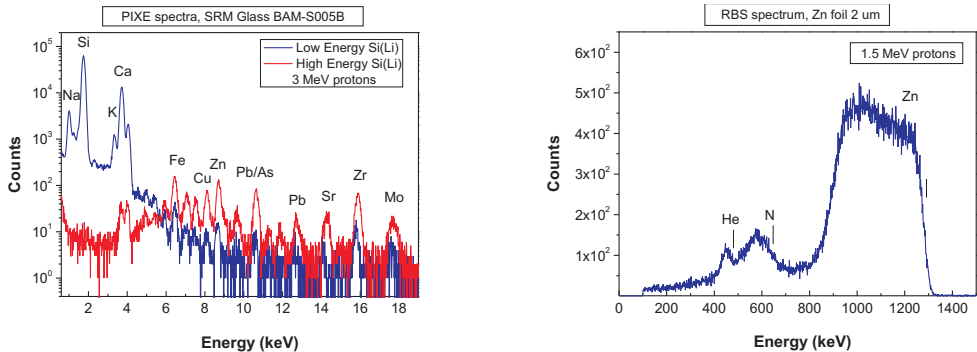


Fig. 9. PIXE and RBS Spectra recorded with the new experimental setup.

5 Conclusions

The first runs were very promising towards the synergistic use of PIXE, RBS and PIGE techniques, confirming a good precision of the measurements and of the integrated analytical capabilities of the set-up. The runs indicate that the proper study/design of the experimental setup provides optimum detection capabilities (elemental sensitivity down to a few ppm) that in combination with the setup precision results in a powerful analytical tool.

6 Acknowledgments

The work was funded by the program ATT_29, PEP Attikis, entitled Embedded elemental tagging technologies and non- destructive techniques for authentication and identity verification of archaeological artifacts, works of art and museum quality technologically authentic copies., co- funded by the Greek General Secretariat of Research and Technology, Ministry of Development and EU.

References

- [1] T. Calligaro, J.-C. Dran, J. Salomon, Ph. Walter, Nucl. Instr.and Meth. B 226, 29, (2004).
- [2] Mando, P.A., Nuclear Physics A 751 (1-4 SPEC. ISS.), pp. 393c-408c (2005)
- [3] Mando, P.A. , Nuovo Cimento della Societa Italiana di Fisica C 30 (1), pp. 85-92 (2007)
- [4] M.A. Respaldiza, F.J. Ager, A. Carmon, J. Ferrer, M. Garca-Len, J. Garca-Lpez, I. Garca-Orellana, B. Gmez-Tubo, Y. Morilla, M.A. Ontalba and I. Ortega-Feliu, Nuclear Instruments and Methods in Physics Research, Section B: Beam Interactions with Materials and Atoms 266 (10), pp. 2105-2109 (2008)